


## Generalized Ornstein-Uhlenbeck model for active motion

Francisco J. Sevilla <sup>1,\*</sup>, Rosalío F. Rodríguez,<sup>1,2</sup> and Juan Ruben Gomez-Solano<sup>1</sup>

<sup>1</sup>*Departamento de Sistemas Complejos, Instituto de Física, Universidad Nacional Autónoma de México, Apdo. Postal 20-364, 01000, Ciudad de México, México*

<sup>2</sup>*FENOMECE, Universidad Nacional Autónoma de México, Apdo. Postal 20-726, 01000, Ciudad de México, México*



(Received 24 May 2019; published 16 September 2019)

We investigate a one-dimensional model of active motion, which takes into account the effects of persistent self-propulsion through a memory function in a dissipative-like term of the generalized Langevin equation for particle swimming velocity. The proposed model is a generalization of the active Ornstein-Uhlenbeck model introduced by G. Szamel [*Phys. Rev. E* **90**, 012111 (2014)]. We focus on two different kinds of memory which arise in many natural systems: an exponential decay and a power law, supplemented with additive colored noise. We provide analytical expressions for the velocity autocorrelation function and the mean-squared displacement, which are in excellent agreement with numerical simulations. For both models, damped oscillatory solutions emerge due to the competition between the memory of the system and the persistence of velocity fluctuations. In particular, for a power-law model with fractional Brownian noise, we show that long-time active subdiffusion occurs with increasing long-term memory.

DOI: [10.1103/PhysRevE.100.032123](https://doi.org/10.1103/PhysRevE.100.032123)

### I. INTRODUCTION

Systems in out-of-equilibrium conditions are ubiquitous in nature, among which biological active matter is the most representative. For instance, motile bacteria employ diverse swimming patterns to traverse complex habitats [1,2]. Recent technological advances have allowed the design of artificial particles that take advantage of different physical and/or chemical mechanisms to self-induce motion that mimics biological motility [3]. Such mobile entities, either biological [4,5] or human-made [6–10], are able to develop autonomously directed motion by using the locally available energy from the environment [3]. These particles are called *self-propelled* or, more generally, *active particles*.

For nonequilibrium statistical physicists, active matter provides a rich field of research that has allowed the rapid progress of different theoretical frameworks. It has been pointed out that the detailed balance between the injection and the dissipation of energy is not satisfied at the microscopic scale in active systems. However, many of the accomplished advancements in the understanding of active matter have partly relied on the intuition built from equilibrium systems [11–13]. For instance, the concept of *effective temperature* has provided a valuable description of some out-of-equilibrium systems [14–16], and in particular in systems of active particles [7,17–24]. In general, the possibility of defining an effective temperature relies on the fulfillment of a nonthermal fluctuation-dissipation relation. This is the case for timescales larger than the persistence one, for which the motion of free active particles is well characterized by an effective diffusion coefficient. Such a behavior can be interpreted as the motion of a passive Brownian particle diffusing in a *fictitious*

environment at an effective temperature higher than the true equilibrium temperature of the surroundings.

A model of active motion that has attracted a great deal of attention because of its simplicity is the so-called *active Ornstein-Uhlenbeck model* (AOUM). It is based on the assumptions that in the overdamped regime, the particle position changes in time due to all the potentials that affect its motion, as well as due to its own self-propulsion velocity, which is described by an Ornstein-Uhlenbeck process [22]. The AOUM has been used as a basis to consider interactions among self-propelled particles [25,26] and to study the main nonequilibrium features exhibited by active matter, such as *motility-induced phase separation* [27,28]. Also, it has allowed the derivation of analytical results in the case of independent active particles confined in simple potentials [29,30]. Furthermore, within the framework of stochastic thermodynamics, it has permitted the analysis of entropy production, fluctuation theorems, and Clausius relations for active matter [31–33].

In this paper we consider a generalization of the AOUM based on the *generalized Langevin equation* (GLE) [34,35], which endows the standard Langevin model of Brownian motion with finite-time correlations. The GLE usually models systems in viscoelastic baths near equilibrium states and includes retarded memory effects in the viscous drag term of the equation and correlated thermal noises [36–43]. Remarkably, these kinds of models are also of great theoretical interest to describe nonequilibrium systems, as memory effects cannot be neglected in many situations. For active matter, memory effects can significantly alter the directional dynamics of individual self-propelled particles when moving in viscoelastic media. For instance, in polymer solutions the persistence length of flagellated bacteria [44] and synthetic nanopropellers [45] is enhanced, while self-propelled spherical colloids exhibit an increase of rotational diffusion [46] and circular trajectories [47]. Memory effects are revealed in many

\*Corresponding author: [fjsevilla@fisica.unam.mx](mailto:fjsevilla@fisica.unam.mx)

other active systems with long-range temporal correlations that also motivate our analysis, e.g., self-propelled particles in glassy [48] or disordered heterogeneous media [49,50], motile bacteria with intricate swimming patterns [1], microorganisms with strong autochemotactic response [51], and active liquid-crystal droplets [52].

In Sec. II we present the explicit formulation of the model that describes the motion of self-propelled particles subject to thermal and active fluctuations. We show that the probability density of the complete process can be written as the convolution of the diffusion probability density, due to thermal fluctuations, and the corresponding probability distribution of the active part of motion, which is analyzed in Sec. III. In the same section two relevant examples are discussed in detail, first, a memory function that models the retarded effects on the swimming velocity due to viscoelastic-like effects, and, second, a memory function with power-law long-lived correlations. Both examples qualitatively capture the phenomenology observed in a variety of active systems, namely the occurrence of anticorrelations of the swimming velocity which lead to self-trapping effects. Finally, in Sec. IV we summarize the main results of our work and make some further physical remarks.

## II. THE GENERALIZED ORNSTEIN-UHLENBECK MODEL OF ACTIVE MOTION

One remarkable aspect of the motion of active particles is that it is *persistent*, i.e., the particles approximately retain the state of motion for a characteristic finite timescale, called the *persistence time*. This feature is indeed observed in the patterns of motion of different microorganisms and some artificially designed self-motile particles. For instance, the *run-and-tumble* pattern of *Escherichia coli* alternates time intervals at a rather constant speed in a straight line along a randomly chosen direction, interrupted by short time periods during which the bacterium tumbles almost at rest. On a statistical description, the run-and-tumble motion can be characterized by a finite timescale of persistence, which makes the motility behavior strongly correlated in time, thus rendering the nonequilibrium signatures conspicuously observable.

Here we provide a theoretical framework with the possibility of considering a variety of patterns of persistent motion. The equations that describe the time evolution of the particle position  $x(t)$  of an overdamped active Brownian particle diffusing in one dimension, and the time evolution of its swimming velocity,  $v_s(t)$ , are given by

$$\frac{d}{dt}x(t) = v_s(t) + \xi_x(t), \quad (1a)$$

$$\frac{d}{dt}v_s(t) = -\frac{1}{\tau_R} \int_0^t ds \gamma(t-s)v_s(s) + \xi_{v_s}(t). \quad (1b)$$

In Eq. (1a),  $\xi_x(t)$  denotes the thermal noise caused by the medium, which is modeled here as Gaussian white noise, i.e., with average  $\langle \xi_x(t) \rangle = 0$  and autocorrelation function  $\langle \xi_x(t)\xi_x(s) \rangle = 2D_T\delta(t-s)$ ;  $D_T$  is the diffusion constant due to translational motion given by  $\mu k_B T$ ,  $\mu$  being the mobility;  $k_B$  the Boltzmann constant; and  $T$  the medium temperature. Equation (1b) is the well-known GLE that in the context of the present paper provides a generalization of the AOUM of

active motion [22], which takes into account the exponential correlations of the swimming velocity that gives rise to exponentially persistent motion. Here, Eq. (1b) opens the door for taking into account a variety of persistent motions by properly choosing the memory function  $\gamma(t)$  [53], which has units of  $\text{time}^{-1}$ . The timescale  $\tau_R$  in Eq. (1b) characterizes the persistence of the velocity fluctuations (the *persistence time*). For times larger than  $\tau_R$ , they relax to zero, fading out the ballistic motion.

We focus on the physically relevant case where Eqs. (1) describe a stationary process whose statistical properties are invariant under temporal translations. For simplicity, the *noise* term  $\xi_{v_s}(t)$  is assumed to be stationary and Gaussian with vanishing average  $\langle \xi_{v_s}(t) \rangle = 0$  and autocorrelation function

$$\langle \xi_{v_s}(t)\xi_{v_s}(s) \rangle = \frac{v_0^2}{\tau_R} \eta(|t-s|). \quad (2)$$

In Eq. (2),  $\eta(t)$  is a function with physical units of  $\text{time}^{-1}$ , whereas  $v_0$  determines the variance of the velocity fluctuations,  $\langle v_s(t)v_s(t) \rangle = \langle v_s(0)v_s(0) \rangle = v_0^2$ , which defines the *characteristic self-propelling speed*  $v_0$ . Although there are no *a priori* reasons to establish a relation between  $\gamma(t)$  and  $\eta(t)$ , it is physically plausible that the relation  $\eta(t) = \gamma(t)$  may be sustained in some cases of interest. This relation does not imply thermal equilibrium but only expresses the simple situation, described by linear-response theory, for which the response of the swimming velocity to active fluctuations is connected by the square of the self-propelling speed divided by the persistent time [54]. The active Ornstein-Uhlenbeck model of Szamel [22] is recovered from Eq. (1b) for the zero-ranged memory function  $\gamma(t) = \eta(t) = 2\delta(t)$ , which leads to an exponentially decaying autocorrelation function, i.e.,  $\langle v_s(t)v_s(s) \rangle = v_0^2 \exp(-|t-s|/\tau_R)$ , also considered in the analysis of a two-dimensional active motion in Ref. [55].

We pay particular attention to the statistical properties of active motion induced by finite- and long-ranged memory functions. We are mainly interested on the statistics of the particle swimming velocity and its position, for which the explicit dynamics of the self-propulsion velocity is implied by the memory function  $\gamma(t)$ . The formal solutions of Eqs. (1) are given explicitly by

$$x(t) = \langle x(t) \rangle + \int_0^t ds \Gamma(t-s)\xi_x(s) + \int_0^t ds \xi_x(s), \quad (3a)$$

$$v_s(t) = \langle v_s(t) \rangle + \int_0^t ds \Gamma'(t-s)\xi_{v_s}(s), \quad (3b)$$

where

$$\langle x(t) \rangle = x(0) + v_s(0) \Gamma(t), \quad (4a)$$

$$\langle v_s(t) \rangle = v_s(0) \Gamma'(t), \quad (4b)$$

give the mean position and the mean swimming velocity, respectively. The average  $\langle \cdot \rangle$  is taken over the independent realizations of the Gaussian white noises  $\xi_x(t)$  and  $\xi_{v_s}(t)$ , while  $\langle \cdot \rangle$  only over realizations of  $\xi_{v_s}(t)$ .  $x(0)$  and  $v_s(0)$  are the corresponding initial values.  $\Gamma(t)$  and  $\Gamma'(t) = d\Gamma(t)/dt$

are the solutions of the deterministic counterpart of Eqs. (1a) and (1b) and given by the inverse Laplace transform of

$$\tilde{\Gamma}(\epsilon) = \epsilon^{-1} \tilde{\Gamma}'(\epsilon), \quad (5a)$$

$$\tilde{\Gamma}'(\epsilon) = \left[ \epsilon + \frac{1}{\tau_R} \tilde{\gamma}(\epsilon) \right]^{-1}, \quad (5b)$$

respectively. The symbol  $\tilde{f}(\epsilon)$  denotes the Laplace transform of the function of time  $f(t)$ , defined by  $\tilde{f}(\epsilon) = \int_0^\infty dt e^{-\epsilon t} f(t)$  with  $\epsilon$  the Laplace variable, a complex number.

The long-time regime of the quantities (5) is determined by the asymptotic behavior of  $\gamma(t)$ . It is customary to require that  $\gamma(t)$  vanishes with increasing  $t$ , which means that in the Laplace domain  $\lim_{\epsilon \rightarrow 0} \epsilon \tilde{\gamma}(\epsilon) \rightarrow 0$ . A necessary and sufficient condition for a well-defined asymptotic limit of  $\Gamma(t)$  and  $\Gamma'(t)$ , and therefore a well-behaved time dependence of the average trajectories (4), is that  $\epsilon \tilde{\gamma}(\epsilon)$  goes to zero slower than  $\epsilon^2$ . This is trivially satisfied by positive monotonically decreasing memory functions—which maintain the physical interpretation of persistence—that go exponentially or faster to zero or by those that go to zero as  $t^{-\beta}$  with  $0 < \beta < 1$ .

The characteristic function of the probability density associated to the stochastic process defined by Eqs. (1) is given by

$$\begin{aligned} \hat{G}(k, q, t) = & \left\langle \left\langle \exp \left\{ -i \int_0^t ds k \xi_x(s) \right\} \right. \right. \\ & \left. \left. \times \exp \left\{ -i \int_0^t ds [q \Gamma'(t-s) + k \Gamma(t-s)] \xi_{v_s}(s) \right\} \right\rangle \right\rangle. \end{aligned} \quad (6)$$

This quantity can be explicitly written as the product of the characteristic function of the translational part  $\hat{G}_{D_T}(k, t)$  times the corresponding bivariate characteristic function of the active part  $\hat{G}_{\text{act}}^{(2)}(k, q, t)$ , i.e.,

$$\hat{G}(k, q, t) = \hat{G}_{D_T}(k, t) \hat{G}_{\text{act}}^{(2)}(k, q, t), \quad (7)$$

where

$$\hat{G}_{D_T}(k, t) = \exp\{-D_T k^2 t\} \quad (8a)$$

is the univariate characteristic function of the diffusion equation,  $D_T$  the diffusion coefficient linked to thermal fluctuations, and

$$\hat{G}_{\text{act}}^{(2)}(k, q, t) = \exp \left[ -\frac{1}{2} q^2 \sigma_{v_s}^2(t) - q k \sigma_{xv_s}^2(t) - \frac{1}{2} k^2 \sigma_{xx}^2(t) \right] \quad (8b)$$

is a bivariate Gaussian that corresponds to the characteristic function of active motion. The expression for  $\hat{G}_{\text{act}}^{(2)}(k, q, t)$  in Eq. (8b) explicitly involves the standard elements of the active covariance matrix  $\Sigma_{\text{act}}$ , i.e., the variance of the particle position  $\sigma_{xx}^2(t) \equiv \langle [x(t) - \langle x(t) \rangle]^2 \rangle$ , the variance of the particle swimming velocity  $\sigma_{v_s}^2(t) \equiv \langle [v_s(t) - \langle v_s(t) \rangle]^2 \rangle$ , and the covariance of the particle position and swimming

velocity  $\sigma_{xv_s}^2 \equiv \langle [x(t) - \langle x(t) \rangle][v_s(t) - \langle v_s(t) \rangle] \rangle$ . Such matrix elements are given by

$$\sigma_{v_s}^2(t) = \frac{v_0^2}{\tau_R} \int_0^t ds_1 \int_0^t ds_2 \Gamma'(s_1) \Gamma'(s_2) \eta(|s_1 - s_2|), \quad (9a)$$

$$\sigma_{xx}^2(t) = \frac{v_0^2}{\tau_R} \int_0^t ds_1 \int_0^t ds_2 \Gamma(s_1) \Gamma(s_2) \eta(|s_1 - s_2|), \quad (9b)$$

$$\sigma_{xv_s}^2(t) = \frac{v_0^2}{\tau_R} \int_0^t ds_1 \int_0^t ds_2 \Gamma'(s_1) \Gamma(s_2) \eta(|s_1 - s_2|), \quad (9c)$$

and are valid for arbitrary  $\gamma(t)$  and  $\eta(t)$ .

Thus, the joint probability density of finding a particle at position  $x$  and swimming with velocity  $v_s$  at time  $t$ , given that initially ( $t = 0$ ) the particle was located at  $x(0)$  swimming at velocity  $v_s(0)$ ,  $P[x, v_s, t | x(0), v_s(0)]$ , can be written as the convolution

$$\begin{aligned} P[x, v_s, t | x(0), v_s(0)] = & \int_{-\infty}^{\infty} dx' G_{D_T}[x - \langle x(t) \rangle - x', t] \\ & \times G_{\text{act}}^{(2)}[x', v_s - \langle v_s(t) \rangle, t], \end{aligned} \quad (10)$$

where

$$G_{D_T}(x, t) = \frac{1}{\sqrt{4\pi D_T t}} \exp\left(-\frac{x^2}{4D_T t}\right) \quad (11)$$

is obtained straightforwardly by inverting the Fourier transform of Eq. (8a), while

$$\begin{aligned} G_{\text{act}}^{(2)}(x, v_s, t) = & \frac{1}{2\pi \sigma_{xx}(t) \sigma_{v_s v_s}(t) \sqrt{1 - C(t)}} \\ & \times \exp \left\{ -\frac{1}{2[1 - C(t)]} \left[ \frac{v_s^2}{\sigma_{v_s v_s}^2(t)} - \frac{2xv_s C(t)}{\sigma_{xv_s}^2(t)} \right. \right. \\ & \left. \left. + \frac{x^2}{\sigma_{xx}^2(t)} \right] \right\} \end{aligned} \quad (12)$$

is obtained after inverting the Fourier transform of (8b), where

$$C(t) = \frac{\sigma_{xv_s}^2(t) \sigma_{v_s v_s}^2(t)}{\sigma_{v_s v_s}^2(t) \sigma_{xx}^2(t)}. \quad (13)$$

### III. THE STATISTICS OF THE ACTIVE COMPONENT OF MOTION

We have shown that the dynamics is explicitly split into the translational part and the active one [see Eqs. (7) and (10)]. This allows us to focus on the statistical properties of the active part of motion. In such a case, it is equivalent to consider Eq. (1) with  $D_T = 0$  [ $\xi_x(t) = 0$  for all  $t$ ], which reduces to the standard generalized Langevin equation that describes the persistence effects of active motion through the memory function in the dissipative term [53]. In order to unveil the main consequences of the model proposed, we restrict our analysis to the case of internal noise, i.e.,  $\eta(t) = \gamma(t)$ .

In addition to the quantities given in Eqs. (9) [evaluated at  $\eta(t) = \gamma(t)$ ], we consider the autocorrelation function of the

swimming velocity  $\langle v_s(t)v_s(s) \rangle$  which can be written as

$$\begin{aligned} \langle v_s(t)v_s(s) \rangle &= v_s^2(0)\Gamma'(t)\Gamma'(s) \\ &+ \frac{v_0^2}{\tau_R} \int_0^t ds_1 \int_0^s ds_2 \Gamma'(s_1)\Gamma'(s_2)\gamma(|s_1 - s_2|) \end{aligned} \quad (14)$$

for  $s \leq t$ .

The asymptotic behavior of the quantities (9) and (14) is determined by the corresponding one of  $\gamma(t)$ , which is deduced by requiring a well-behaved time dependence of  $\Gamma(t)$  and  $\Gamma'(t)$ . Such behavior is fulfilled if (a)  $\gamma(t)$  vanishes exponentially or faster or if (b) it vanishes as  $t^{-\beta}$  with  $0 < \beta < 1$ . In any case we have that  $\sigma_{v_s v_s}^2(t) \rightarrow 2v_0^2$ , while it can be shown that for case (a) we have  $\sigma_{xx}^2(t) \rightarrow 2v_0^2\tau_R t$ , from which the active diffusion coefficient  $D = v_0^2\tau_R$  is evident and  $\sigma_{xv_s}^2(t) \rightarrow v_0^2\tau_R$ . For the case (b) we have  $\sigma_{xx}^2(t) \rightarrow 2v_0^2\tau_R(\gamma_0 t)^\beta/\Gamma(\beta+1)\gamma_0$  and  $\sigma_{xv_s}^2(t) \rightarrow v_0^2\tau_R(\gamma_0 t)^{\beta-1}/\Gamma(\beta)$ .  $\gamma_0^{-1}$  is a timescale that characterizes the memory function and the relation  $\sigma_{xv_s}^2(t) = (1/2)(d/dt)\sigma_{xx}^2(t)$  has been used.

Furthermore, in striking contrast with the zero-ranged memory function, which gives rise to positive correlations of the swimming velocity and to a smooth crossover between the ballistic superdiffusion and the normal diffusion, finite-ranged memory functions lead to anticorrelations of the swimming velocity in the intermediate-time regime. These anticorrelations are conspicuously revealed in the intermediate-time regime of  $\sigma_{xx}^2(t)$ , which are interpreted as a *self-trapping effect*. This is discussed in detail in the following subsections.

The corresponding joint probability density of the active part of motion,  $P_{\text{act}}[x, v_s, t|x(0), v_s(0)]$ , is given by the convolution of  $G_{\text{act}}^{(2)}(x, v_s, t)$  with the joint density induced by the deterministic part of Eqs. (3), namely

$$\begin{aligned} &\int_{-\infty}^{\infty} dx' \int_{-\infty}^{\infty} dv'_s G_{\text{act}}^{(2)}(x-x', v_s-v'_s, t) \\ &\times \delta[x' - \langle x(t) \rangle] \delta[v'_s - \langle v_s(t) \rangle]. \end{aligned} \quad (15)$$

Using the characteristic function method [56], one can easily show that  $G_{\text{act}}^{(2)}(x, v_s, t)$  satisfies the Fokker-Planck equation (see Appendix A),

$$\begin{aligned} &\left( \frac{\partial}{\partial t} + v_s \frac{\partial}{\partial x} \right) G_{\text{act}}^{(2)}(x, v_s, t) \\ &= \left[ f(t) \frac{\partial}{\partial v_s} v_s + g(t) \frac{\partial^2}{\partial x \partial v_s} + h(t) \frac{\partial^2}{\partial v_s^2} \right] G_{\text{act}}^{(2)}(x, v_s, t), \end{aligned} \quad (16)$$

where

$$f(t) = \frac{\sigma_{v_s v_s}^2(t)}{\sigma_{xv_s}^2(t)}, \quad (17a)$$

$$g(t) = \frac{d}{dt} \sigma_{xv_s}^2(t), \quad (17b)$$

$$h(t) = \frac{1}{2} \frac{d}{dt} \sigma_{v_s v_s}^2(t) + \frac{[\sigma_{v_s v_s}^2(t)]^2}{\sigma_{xv_s}^2(t)}. \quad (17c)$$

In the following subsections we analyze the consequences of the present model by considering an instance of interest for each of the two asymptotic behaviors of  $\gamma(t)$  considered in

this paper. The first example considers a memory function that decays at least exponentially faster, while the second assumes the asymptotic behavior of a power law.

### A. Exponential memory kernel

As a first example, we focus on a memory kernel consisting of a  $\delta$  function plus an exponential decay with relaxation time  $\tau$  [57],

$$\gamma(t) = 2(1-\alpha)\delta(t) + \frac{\alpha}{\tau} \exp\left(-\frac{|t|}{\tau}\right), \quad (18)$$

where  $0 < \alpha < 1$  is a dimensionless parameter that weighs the role of the exponential memory over the  $\delta$  one. This kind of memory kernel describes the rheological response of several viscoelastic materials, such as intracellular fluids [58], polymer solutions [59], wormlike micelles [60], and  $\lambda$ -phage DNA [61], where  $\tau$  is the relaxation time of the elastic microstructure [62]. In the present work, it represents the retarded effects on the swimming velocity due to viscoelastic-like effects. More precisely, it considers two channels of persistence: the standard one, given by the  $\delta$  function and considered in Ref. [22], that leads to exponentially decaying correlations of the swimming velocity, and the other one leads to long-lived correlations exhibiting intermittently negative correlations in the intermediate-time regime. For either  $\alpha = 0$  or  $\tau \rightarrow 0$ , Eq. (18) corresponds to the AOUM of Szamel [22].

In order to simulate trajectories evolving according to the generalized model presented in this paper, for  $0 < \alpha < 1$ , we express Eq. (1b) in a Markovian form by introducing the additional variable

$$u(t) = \frac{1}{\tau} \int_0^t ds \exp\left(-\frac{t-s}{\tau}\right) [v_s(s) + \tau\phi_2(s)], \quad (19)$$

where  $\phi_2$  is a zero-mean Gaussian noise with autocorrelation

$$\langle \phi_2(t)\phi_2(s) \rangle = \frac{2v_0^2\tau_R}{\alpha\tau^2} \delta(t-s). \quad (20)$$

Then, Eq. (1b) can be written as

$$\frac{d}{dt} v_s(t) = -\frac{1-\alpha}{\tau_R} v_s(t) - \frac{\alpha}{\tau_R} u(t) + \phi_1(t), \quad (21a)$$

$$\frac{d}{dt} u(t) = -\frac{1}{\tau} [u(t) - v_s(t)] + \phi_2(t), \quad (21b)$$

where  $\phi_1(t)$  is a zero-mean Gaussian noise, which satisfies

$$\langle \phi_1(t)\phi_1(s) \rangle = \frac{2(1-\alpha)v_0^2}{\tau_R} \delta(t-s). \quad (22)$$

In the following, length scales are normalized by the *persistence length*  $v_0\tau_R$ , timescales by  $\tau_R$ , velocities by  $v_0$ , and translational diffusion coefficients by  $v_0^2\tau_R$ . In Fig. 1(a) we plot some simulated trajectories for different values of the memory  $\tau$  and constant  $\alpha = 0.9$ . As  $\tau$  increases, the shape of the trajectories change qualitatively, displaying three distinct kinds of behaviors. To better appreciate such regimes for different values of  $\tau$ , we compute the corresponding velocity autocorrelation function  $\langle v_s(t)v_s(0) \rangle$ . In accordance with our linear-response assumption, this is given by  $v_0^2\Gamma'(t)$  [see Eq. (14)], where  $\Gamma'(t)$  has been introduced in Eqs. (3b) and (4b) and defined in Eq. (5b). As shown in Fig. 1(b), for

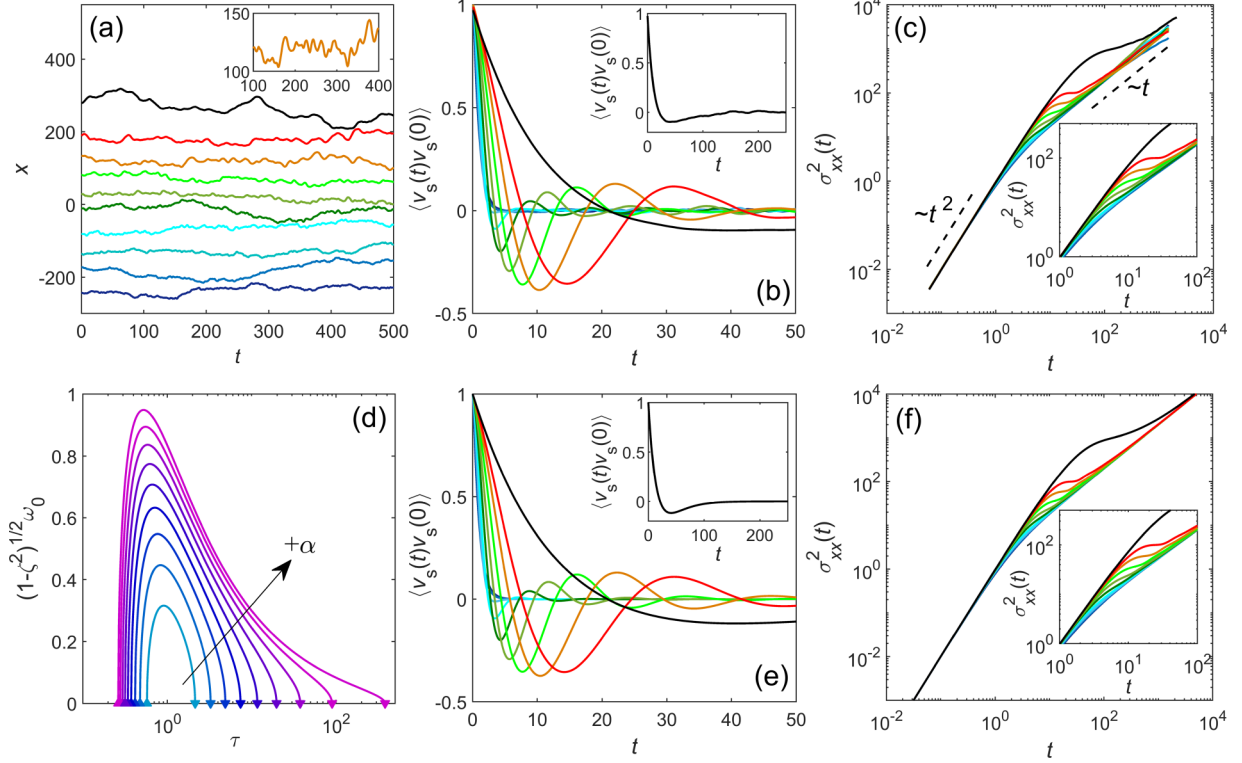


FIG. 1. (a) Examples of trajectories  $x(t)$  evolving according to the generalized Ornstein-Uhlenbeck model (1), with memory kernel given by (18), for  $\alpha = 0.9$  and different values of the memory time  $\tau$ . From bottom to top:  $\tau = 0.1, 0.2, 0.4, 0.8, 1.6, 3.2, 6.4, 12.8, 25.6, 400$ . Inset: Expanded view the active trajectory with  $\tau = 12.8$ . (b) Corresponding velocity autocorrelation function for different values of  $\tau$ , same color code as in (a). The values of  $\tau$  increase from left to right. Inset: Expanded view for  $\tau = 400$ . (c) Mean-squared displacements of the trajectories shown in (a). The values of  $\tau$  increase from bottom to top. Inset: Expanded view of the intermediate regime around  $\tau_R$ . (d) Dependence on the relaxation time  $\tau$  of the frequency of the damped oscillations, which emerge only between  $\tau_+$  ( $\Delta$ ) and  $\tau_-$  ( $\nabla$ ), for different values of  $\alpha$  increasing from inner to outer curves:  $\alpha = 0.1, 0.2, 0.3, 0.4, 0.5, 0.6, 0.7, 0.8, 0.9$ . (e) Velocity autocorrelation function and (f) mean-squared displacement, obtained from the analytical expression, for the same parameters plotted in (b) and (c), respectively.

small values of  $\tau$  ( $\tau = 0.1$  and  $\tau = 0.2$ ) the velocity autocorrelation function  $\langle v_s(t)v_s(0) \rangle$  exhibits a monotonic decay. Furthermore, damped oscillations of  $\langle v_s(t)v_s(0) \rangle$  show up at larger  $\tau$ , thus manifesting the appearance of anticorrelations with a frequency that strongly depends on  $\tau$ , as observed for  $0.4 \leq \tau \leq 25.6$ . For instance, in the inset of Fig. 1(a), such oscillations can be clearly observed along an active trajectory with  $\tau = 12.8$ . Moreover, the oscillations vanish at very large  $\tau$ , where  $\langle v_s(t)v_s(0) \rangle$  exhibits a single global minimum, as shown in the inset of Fig. 1(b) for  $\tau = 400$ , where velocity anticorrelations occur. In Fig. 1(c) we show the resulting mean-squared displacements  $\sigma_{xx}^2(t)$ . For all values of the relaxation time  $\tau$ , a ballistic  $\sigma_{xx}^2(t) \propto t^2$  and diffusive regime  $\sigma_{xx}^2(t) \propto t$  is observed on timescales  $t \ll \tau_R$  and  $t \gg \tau_R$ , respectively. This is in contrast to intermediate timescales (comparable to  $\tau_R$ ), where a strong dependence on  $\tau$  is found, see inset of Fig. 1(c).

Indeed, from Eqs. (21), we can derive the following equation for the autocorrelation function:

$$\begin{aligned}
 \frac{d^2 \langle v_s(t)v_s(0) \rangle}{dt^2} + \left( \frac{1}{\tau} + \frac{1-\alpha}{\tau_R} \right) \frac{d \langle v_s(t)v_s(0) \rangle}{dt} \\
 + \frac{1}{\tau \tau_R} \langle v_s(t)v_s(0) \rangle = 0,
 \end{aligned} \quad (23)$$

which is formally equivalent to the equation of motion of a damped harmonic oscillator with undamped angular frequency  $\omega_0$  and damping ratio  $\zeta$  given by

$$\omega_0 = \frac{1}{\sqrt{\tau \tau_R}}, \quad (24a)$$

$$\zeta = \frac{1}{2} \sqrt{\tau \tau_R} \left( \frac{1}{\tau} + \frac{1-\alpha}{\tau_R} \right), \quad (24b)$$

respectively. Under the initial conditions  $\langle v_s(0)v_s(0) \rangle = v_0^2$  and  $\frac{d \langle v_s(t)v_s(0) \rangle}{dt} \Big|_{t=0} = -\frac{1-\alpha}{\tau_R} v_0^2$ , Eq. (23) has three different kinds of solutions, which are determined by two particular values of the memory time  $\tau$

$$\tau_+ = \frac{\tau_R}{(1 + \sqrt{\alpha})^2}, \quad (25a)$$

$$\tau_- = \frac{\tau_R}{(1 - \sqrt{\alpha})^2}. \quad (25b)$$

Note that  $\tau_+ < \tau_R$ , whereas  $\tau_- > \tau_R$  for all values of  $\alpha$ . In particular, for the value  $\alpha = 0.9$  considered here in most of our numerical results,  $\tau_+ = 0.26$  and  $\tau_- = 379.74$ . For  $0 \leq \tau < \tau_+$  or  $\tau_- < \tau$ , the solution for  $\langle v_s(t)v_s(0) \rangle$  is composed

of two exponential decays,

$$\langle v_s(t)v_s(0) \rangle = \frac{v_0^2}{2\omega_0\sqrt{\zeta^2-1}} \left[ A_- e^{-\omega_0(\zeta-\sqrt{\zeta^2-1})t} + A_+ e^{-\omega_0(\zeta+\sqrt{\zeta^2-1})t} \right], \quad (26)$$

where the amplitudes  $A_{\pm}$  are given by

$$A_{\pm} = \frac{1}{2} \sqrt{\left( \frac{1-\alpha}{\tau_R} + \frac{1}{\tau} \right)^2 - \frac{4}{\tau\tau_R}} \pm \frac{1}{2} \left( \frac{1-\alpha}{\tau_R} - \frac{1}{\tau} \right). \quad (27)$$

For  $0 \leq \tau < \tau_+$ , Eq. (26) represents a double-exponentially monotonic decay from  $v_0^2$  to 0 of the velocity autocorrelation function. This corresponds to the behavior shown in Fig. 1(b) for  $\tau = 0.1$  and  $0.2$ , which are below  $\tau_+$ . On the other hand,  $\tau_- < \tau$  yields a nonmonotonic dependence of  $\langle v_s(t)v_s(0) \rangle$  on  $t$ , with a single minimum around which anticorrelations  $\langle v_s(t)v_s(0) \rangle < 0$  happen. This is illustrated in the inset of Fig. 1(b) for  $\tau = 400$ , where  $\langle v_s(t)v_s(0) \rangle < 0$  for  $t > 20.89$ , while the minimum is located at  $t = 40.72$ .

At  $\tau = \tau_{\pm}$ , the velocity autocorrelation function takes the critical damping form

$$\langle v_s(t)v_s(0) \rangle = v_0^2 e^{-\frac{t}{\sqrt{\tau_{\pm}\tau_R}}} \left[ 1 + \left( \frac{1}{\sqrt{\tau_{\pm}\tau_R}} - \frac{1-\alpha}{\tau_R} \right) t \right]. \quad (28)$$

The two solutions (28) separate the pure exponential solutions for  $0 \leq \tau < \tau_+$  and  $\tau_- < \tau$  from those within the interval  $\tau_+ < \tau < \tau_-$ . For the latter, the velocity autocorrelation function has the following damped-oscillatory form:

$$\langle v_s(t)v_s(0) \rangle = v_0^2 \exp(-\zeta\omega_0 t) [\cos(\sqrt{1-\zeta^2}\omega_0 t) + B \sin(\sqrt{1-\zeta^2}\omega_0 t)], \quad (29)$$

where the amplitude

$$B = \frac{1}{\sqrt{1-\zeta^2}\omega_0} \left( \zeta\omega_0 - \frac{1-\alpha}{\tau_R} \right), \quad (30)$$

and the frequency of the damped oscillations,

$$\sqrt{1-\zeta^2}\omega_0 = \sqrt{\frac{1}{\tau\tau_R} - \frac{1}{4} \left( \frac{1}{\tau} + \frac{1-\alpha}{\tau_R} \right)^2}, \quad (31)$$

has a nonmonotonic dependence on  $\tau$ . This corresponds to the behavior observed for  $\tau = 0.4, 0.8, 1.6, 3.2, 6.4, 12.8$ , and  $25.6$  in Fig. 1(b). In Fig. 1(d) we plot  $\sqrt{1-\zeta^2}\omega_0$  as a function of  $\tau$  for different values of  $\alpha$ . While at small  $\alpha$  the interval over which oscillatory solutions are possible is very narrow and the oscillation frequencies are low, it broadens and the corresponding frequencies are enhanced with increasing  $\alpha$ , i.e., when the exponential memory term in Eq. (18) becomes dominant. In Fig. 1(e) we show the velocity autocorrelation function obtained directly from the explicit expressions (24)–(31) for  $\alpha = 0.9$  and the same values of  $\tau$  as in 1(b), where excellent agreement with the numerical results is observed.

Using the previous expressions for  $\langle v_s(t)v_s(0) \rangle$ , we can readily derive the corresponding ones for the mean-squared

displacement. For  $0 \leq \tau < \tau_+$  or  $\tau_- < \tau$ , this reads

$$\begin{aligned} \sigma_{xx}^2(t) &= 2v_0^2\tau_R [t - (\tau_R - \alpha\tau)] \\ &+ \frac{v_0^2}{\omega_0^2\sqrt{\zeta^2-1}} \left[ C_- e^{-\omega_0(\zeta-\sqrt{\zeta^2-1})t} \right. \\ &\left. + C_+ e^{-\omega_0(\zeta+\sqrt{\zeta^2-1})t} \right], \end{aligned} \quad (32)$$

where

$$C_{\pm} = \pm \frac{-\zeta \pm \sqrt{\zeta^2-1} + \frac{1-\alpha}{\omega_0\tau_R}}{2\zeta(\zeta \pm \sqrt{\zeta^2-1}) - 1}. \quad (33)$$

At  $\tau = \tau_{\pm}$ , the expression for the mean-squared displacement is

$$\begin{aligned} \sigma_{xx}^2(t) &= 2v_0^2\tau_R \left\{ \left[ 1 \pm \frac{\sqrt{\alpha}}{1 \pm \sqrt{\alpha}} \exp\left(-\frac{1 \pm \sqrt{\alpha}}{\tau_R} t\right) \right] t \right. \\ &\left. + \frac{1 \pm 2\sqrt{\alpha}}{(1 \pm \sqrt{\alpha})^2} \tau_R \left[ \exp\left(-\frac{1 \pm \sqrt{\alpha}}{\tau_R} t\right) - 1 \right] \right\}, \end{aligned} \quad (34)$$

while for  $\tau_+ < \tau < \tau_-$ ,  $\sigma_{xx}^2(t)$  can be expressed as

$$\begin{aligned} \sigma_{xx}^2(t) &= 2v_0^2\tau_R \left\{ t - (\tau_R - \alpha\tau) \right. \\ &+ e^{-\zeta\omega_0 t} \left[ \tau_R(\tau_R - \alpha\tau) \cos(\sqrt{1-\zeta^2}\omega_0 t) \right. \\ &\left. \left. - \frac{2\zeta\sqrt{1-\zeta^2} + (1-2\zeta^2)B}{\omega_0^2} \sin(\sqrt{1-\zeta^2}\omega_0 t) \right] \right\}. \end{aligned} \quad (35)$$

Interestingly, mean-squared displacements which are similar to the critical damping (34) and to the damped-oscillatory case (35) have been observed for bacteria with run-reverse-flick swimming [1], for microorganisms with run-reverse locomotion [63], and for more general patterns of active motion [64] or with a strong response to self-produced chemoattractants [51], respectively. In all cases, the previous expressions for the mean-squared displacement reduce to a ballistic regime  $\sigma_{xx}^2(t) \approx v_0^2 t^2$  at short timescales,  $t \ll \tau_R$ . In contrast, at  $t \gg \tau_R$  active diffusion  $\sigma_{xx}^2(t) \approx 2Dt$  is observed, where the active diffusion coefficient is  $D = v_0^2\tau_R$  for all values of  $\tau$ , as shown in Figs. 1(c) for the numerical trajectories and in Fig. 1(f) for the analytical expressions. In the insets of Figs. 1(c) and 1(f), we show that the damped oscillations of  $\langle v_s(t)v_s(0) \rangle$  for  $\tau_+ < \tau < \tau_-$  translate into a shift of the short-time ballistic regime of  $\sigma_{xx}^2(t)$  to timescales larger than  $\tau_R$ . For  $\tau > \tau_-$ , the ballistic behavior of  $\sigma_{xx}^2(t)$  persists for timescales significantly larger than  $\tau_R$ .

The effect of a nonzero thermal diffusion coefficient,  $D_T = k_B T \mu > 0$ , is to simply add an amount  $2D_T t$  to the mean-squared displacement of active motion, which results in a long-time active diffusion with coefficient  $D_T + v_0^2\tau_R$ . Thus, such a diffusive behavior can be interpreted in terms of a nonequilibrium effective temperature  $T_{\text{eff}} = T + \frac{v_0^2\tau_R}{k_B\mu}$ . Note that  $T_{\text{eff}}$  increases quadratically with  $v_0$  regardless of the value of the memory time  $\tau$ . This dependence is similar to that obtained from the conventional AOUM [22] and also to that for active Brownian particles [7].

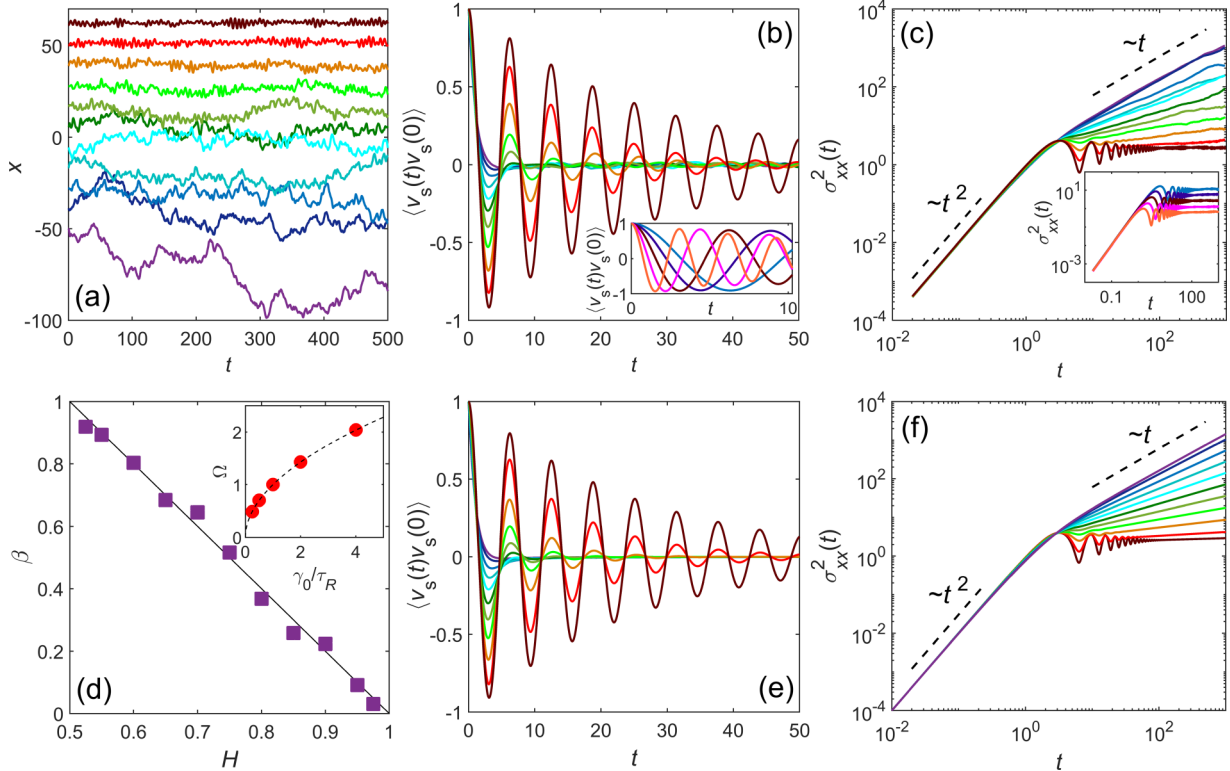


FIG. 2. (a) Examples of trajectories  $x(t)$  evolving according to the generalized Ornstein-Uhlenbeck model (1) with power-law memory kernel (36) and fractional Brownian noise (37) in the absence of thermal fluctuations for different values of the Hurst parameter increasing from bottom to top:  $H = 0.525, 0.55, 0.6, 0.65, 0.7, 0.75, 0.8, 0.85, 0.9, 0.95, 0.975$ . (b) Velocity autocorrelation function and (c) corresponding mean-squared displacement for the different values of the Hurst parameter in (a), same color code. In (b) and (c), the values of  $H$  increase from inner to outer curves and from top to bottom, respectively. The insets in (b) and (c) corresponds to the velocity autocorrelation function and the mean-squared displacement for  $H = 0.975$  and different values of  $\gamma_0/\tau_R$ : from left to right and bottom to top, respectively:  $\gamma_0/\tau_R = 4, 2, 1, 0.5, 0.25$ . (d) Exponent  $\beta$  of the long-time behavior ( $t \gg \tau_R$ ) of the mean-squared displacement as a function of  $H$ . The symbols ( $\square$ ) mark the values obtained from the numerical solutions, whereas the solid line represents  $2 - 2H$ . Inset: Frequency of the velocity oscillations for  $H = 0.975$  as a function of  $\gamma_0/\tau_R$ . The dashed line represents Eq. (42). (e) Velocity autocorrelation function and (f) mean-squared displacement, directly computed from the analytical expressions (40) and (43), respectively, for the same values of  $H$  as those shown in (b) and (c).

### B. Power-law memory kernel

As a second example, we consider a power-law memory kernel [65],

$$\gamma(t) = \frac{\gamma_0 t^{2H-1}}{\Gamma(2H)} \left[ \frac{2H-1}{t} + 2\delta(t) \right], \quad (36)$$

where  $\frac{1}{2} < H < 1$  guarantees the well-behaved time dependence of the quantities in Eqs. (5) and  $\gamma_0 > 0$  a constant with units of  $\text{time}^{1-2H}$ . This kind of memory kernel describes several physical situations, such as the motion of granules within the cytoplasm [66], the micromechanical response of the cytoskeleton [67], and rheological properties of soft biological tissues [68]. In this case, the corresponding stochastic term  $\xi_{v_s}(t)$  in Eq. (1b) is a fractional Gaussian noise (characterized by the Hurst exponent  $H$ ), with autocorrelation function

$$\langle \xi_{v_s}(t) \xi_{v_s}(s) \rangle = \frac{\gamma_0 v_0^2 |t-s|^{2H-1}}{\tau_R \Gamma(2H)} \left[ \frac{2H-1}{|t-s|} + 2\delta(t-s) \right]. \quad (37)$$

Note that this model corresponds to the conventional AOUM [22] if  $H = \frac{1}{2}$ . By integrating Eq. (1b) over the time interval  $[0, t]$ , a straightforward calculation leads to the following

expression for the velocity at time  $t$ :

$$v_s(t) = v_s(0) - \frac{\gamma_0}{\tau_R \Gamma(2H)} \int_0^t ds \frac{v_s(s)}{(t-s)^{1-2H}} + \chi(t), \quad (38)$$

where  $\chi(t) = \int_0^t dt' \xi_{v_s}(t')$  is a fractional Brownian motion [69], which satisfies  $\langle \chi(t) \rangle = 0$  and

$$\langle \chi(t) \chi(s) \rangle = \frac{\gamma_0 v_0^2}{2\tau_R H \Gamma(2H)} (|t|^{2H} + |s|^{2H} - |t-s|^{2H}). \quad (39)$$

We simulate particle trajectories evolving according to this generalized active Ornstein-Uhlenbeck model for different values of the parameters  $H$  and  $\gamma_0/\tau_R$ . To this end, the integral on the right-hand side of Eq. (38) is evaluated using a modified Adams-Bashforth-Moulton algorithm [70], whereas the fractional Brownian motion  $\chi(t)$  is independently generated by means of the circulant embedding method of the covariance matrix [71].

We first study the active motion of a free particle when no translational diffusion ( $D_T = 0$ ) comes into play, i.e.,  $\frac{d}{dt}x(t) = v_s(t)$ . The results for different values of  $H$  are plotted in Figs. 2(a)–2(f), where length scales, timescales, velocities, and translational diffusion coefficients are

normalized by  $v_0\tau_R$ ,  $\tau_R$ ,  $v_0$ , and  $v_0^2\tau_R$ , respectively. Some examples of simulated trajectories  $x(t)$  for different values of  $H$  and  $\gamma_0/\tau_R = 1$  are plotted in Fig. 2(a). We find that with increasing  $H$ , the active trajectories develop a behavior ranging from quasidiffusion at  $H$  slightly larger to  $1/2$  to a strong self-trapping induced by persistent oscillations when  $H$  is close to 1. Indeed, in Fig. 2(b) we observe that the velocity autocorrelation function,  $\langle v_s(t)v_s(0) \rangle$ , exhibits a well-defined oscillatory behavior, alternating between periods of positive correlations and negative correlations, as  $H$  increases. The frequency of the oscillations depends mainly on the parameter  $\gamma_0/\tau_R$ , as confirmed in the inset of Fig. 2(b) for  $H = 0.975$ . This can be understood from the fact that as  $H$  approaches 1, the oscillations emerge from the competition between the long-range persistence of self-propulsion, described by the convolution in Eq. (1b), and the fractional Brownian noise  $\xi_{v_s}$ . Since the intensity of the former is proportional to  $\gamma_0/\tau_R$ , the quantity  $(\tau_R/\gamma_0)^{1/(2H)}$  sets the only characteristic timescale of the system, from which the frequency of the oscillations must be proportional to  $(\gamma_0/\tau_R)^{1/(2H)}$ . Interestingly, the resulting mean-squared displacements display the typical ballistic regime  $\sigma_{xx}^2(t) \propto t^2$  at short timescales  $t \ll \tau_R$  for all  $\frac{1}{2} < H < 1$ , as shown in Fig. 2(c). At larger timescales, the behavior of  $\sigma_{xx}^2(t)$  strongly depends on  $H$ . For instance, for  $H$  larger, but close to  $\frac{1}{2}$ , the mean-squared displacement exhibits approximately the long-time linear behavior expected for active Brownian motion:  $\sigma_{xx}^2(t) \propto t$  for  $t \gg \tau_R$ . As  $H$  increases, an intermediate oscillatory behavior at  $t \gtrsim \tau_R$  shows up, where the amplitude of the oscillations of  $\sigma_{xx}^2(t)$  eventually vanishes and leads to a subdiffusive growth at sufficiently large timescales, confirming the time dependence  $\sigma_{xx}^2(t) \propto t^\beta$ , with  $\beta = 2 - 2H$  as shown in Fig. 2(d). We point out that the previously described behavior is reminiscent of that of soft self-propelled particles with polar alignment in crowded glassy environments [48] and active particles in disordered heterogeneous media [49,50]. In such cases, interparticle and alignment interactions induce long-range temporal correlations in the swimming velocity, which in turn lead to local trapping of the particles, thereby exhibiting transient oscillations followed by long-time subdiffusion.

An analytical expression for the velocity autocorrelation function can be derived from the general solution of Eq. (1b), given by Eqs. (3b), (4b), and (5b). In this case, the Laplace transform of the power-law memory kernel (36) is explicitly given by  $\tilde{\gamma}(\epsilon) = \gamma_0\epsilon^{1-2H}$ . Then a straightforward calculation leads to

$$\langle v_s(t)v_s(0) \rangle = v_0^2 E_{2H,1} \left( -\frac{\gamma_0 t^{2H}}{\tau_R} \right), \quad (40)$$

where  $E_{\mu,\nu}(z)$  is the two-parameter Mittag-Leffler function, defined by the series expansion

$$E_{\mu,\nu}(z) = \sum_{k=0}^{\infty} \frac{z^k}{\Gamma(\mu k + \nu)}, \quad (41)$$

with  $\mu > 0$  and  $\nu > 0$ . In Fig. 2(e) we demonstrate that the velocity autocorrelation curves computed from Eq. (41) reproduce very well the numerical results of Fig. 2(b) for all the values  $H$ . In particular, we note that  $E_{1,1}(z) = \exp(z)$ , while  $E_{2,1}(-z^2) = \cos(z)$ . Therefore, as  $H \rightarrow \frac{1}{2}$ , the velocity

autocorrelation tends to the conventional Ornstein-Uhlenbeck model,  $\langle v_s(t)v_s(0) \rangle = v_0^2 \exp(-\gamma_0 t/\tau_R)$ , with relaxation time  $\tau_R/\gamma_0$ , where  $\gamma_0$  is a dimensionless parameter. On the other hand, as  $H$  approaches 1,  $\langle v_s(t)v_s(0) \rangle$  develops a slow-decaying oscillatory behavior with frequency

$$\Omega = \left( \frac{\gamma_0}{\tau_R} \right)^{\frac{1}{2H}}, \quad (42)$$

in agreement with the frequencies computed numerically, as verified in the inset of Fig. 2(b) for  $H = 0.975$ .

In a similar manner, using the general solution for the particle position given by Eq. (3a), we obtain the following expression for the mean-squared displacement:

$$\sigma_{xx}^2(t) = 2v_0^2 t^2 E_{2H,3} \left( -\frac{\gamma_0 t^{2H}}{\tau_R} \right). \quad (43)$$

Once again, Eq. (43) agrees very well with our numerical results shown in Fig. 2(c) for all  $H$ , see Fig. 2(f). For instance, for  $t \ll (\tau_R/\gamma_0)^{\frac{1}{2H}}$ ,  $E_{2H,3}(-z^{2H}) \approx 1/\Gamma(3) = 1/2$  regardless of  $H$ , and thus Eq. (43) reduces to the short-time ballistic regime,  $\sigma_{xx}^2(t) \approx v_0^2 t^2$ . It should be noted that the oscillations of  $\sigma_{xx}^2(t)$  for  $t > \tau_R$  with increasing  $H$  can only be captured when taking into account the full solution of the velocity autocorrelation function given in terms of the Mittag-Leffler functions, see Eq. (40). The oscillatory behavior of  $\sigma_{xx}^2(t)$  is smeared out by any asymptotic power-law approximation of  $\langle v_s(t)v_s(0) \rangle$ , as those considered in Ref. [56]. Furthermore, taking into account the asymptotic behavior of the general Mittag-Leffler function  $E_{\mu,\nu}(-z) \approx z^{-1}/\Gamma(\nu - \mu)$  for  $z \rightarrow \infty$ , the long-time behavior [ $t \gg (\tau_R/\gamma_0)^{\frac{1}{2H}}$ ] of the mean-squared displacement is [37,53]

$$\sigma_{xx}^2(t) \approx \frac{2v_0^2 \tau_R}{\gamma_0 \Gamma(3 - 2H)} t^{2-2H}, \quad (44)$$

thereby reproducing the exponent  $\beta$  of the active subdiffusive regime we find numerically, see Fig. 2(d). In particular, from Eq. (44) we recover the long-time dependence  $\sigma_{xx}^2(t) \approx 2v_0^2(\tau_R/\gamma_0)t$  as  $H \rightarrow \frac{1}{2}$ , while the active motion is subdiffusive with exponent  $2 - 2H$  for  $H > \frac{1}{2}$ . Total spatial self-trapping occurs for complete persistence, i.e., for  $H = 1$ , for which the mean-squared displacement saturates to the value  $\sigma_{xx}^2(t \rightarrow \infty) = 2v_0^2 \tau_R/\gamma_0$ .

In order to better illustrate the effect of thermal fluctuations on the active trajectories, we focus on a large value of the Hurst parameter ( $H = 0.975$ ), for which the velocity autocorrelation function exhibits a pronounced oscillatory behavior, see Fig. 3(a). The overall effect is that the presence of a nonzero  $D_T > 0$  destroys the long-time subdiffusive behavior, thus leading to trajectories with a large dispersion compared to the diffusion-free case, as shown in Fig. 3(b). In fact, in the presence of translational thermal noise, the mean-squared displacement is supplemented by a diffusive term  $2D_T t$ ,

$$\sigma_{xx}^2(t) = 2v_0^2 t^2 E_{2H,3} \left( -\frac{\gamma_0 t^{2H}}{\tau_R} \right) + 2D_T t. \quad (45)$$

Thus, depending on the value of  $D_T$  and the timescale  $t$ , different regimes are observed. Indeed, in Fig. 3(c), we observe that at short timescales, the mean-squared displacement has a diffusive part (diffusion coefficient equal to  $D_T$ ), because



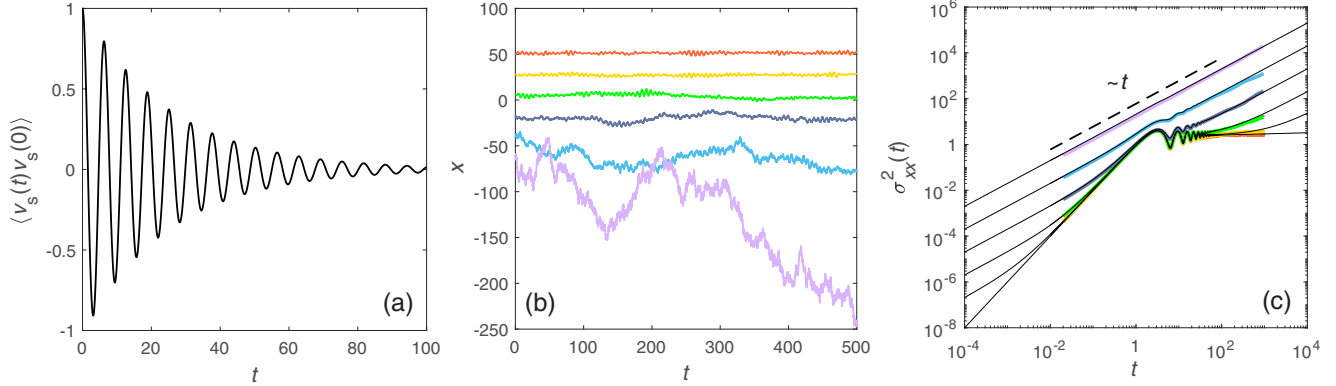


FIG. 3. (a) Velocity autocorrelation function for the active Ornstein-Uhlenbeck model with the power-law memory kernel (36) and fractional Brownian noise at  $H = 0.975$ . (b) Resulting active trajectories for different translational diffusion coefficients from top to bottom:  $D_T = 0, 10^{-3}, 10^{-2}, 10^{-1}, 1, 10$ . (c) Corresponding mean-squared displacements. Same color code as in Fig. 3(b). The values of  $D_T$  increase from bottom to top. The solid lines represent Eq. (45).

the ballistic motion is negligible with respect to thermal diffusion. Furthermore, at sufficiently low  $D_T$ , typically  $D_T \lesssim v_0^2 \tau_R$ , and intermediate timescales (comparable to  $\tau_R$ ), the oscillatory regime is still observed. On the other hand, for a sufficiently large thermal diffusion coefficient ( $D_T \gtrsim v_0^2 \tau_R$ ), diffusion dominates completely the particle motion over all timescales, thereby hindering the memory-induced oscillations. For all values of  $D_T$ , the long-time diffusive behavior occurs, i.e.,  $\sigma_{xx}^2(t) \approx 2D_T t$  for  $t \gg \tau_R$ , due to the dominance of thermal diffusion over the subdiffusive growth  $t^{2-2H}$  in the mean-squared displacement. In all cases, Eq. (45) perfectly describes our numerical results over all timescales and for all values of  $H$ , see solid lines in Fig. 3(c).

We want to point out that in the case of the long-ranged memory kernel considered here, unlike the case of the finite-ranged one given in Eq. (18), the interpretation of the long-time limit of (45) in terms of an effective temperature is less clear. In fact, if  $D_T = 0$ , then an effective temperature cannot be defined in a straightforward manner, mainly due to the long-ranged (anti-)correlations of the swimming velocity that leads to a self-trapping effect and therefore to the subdiffusive behavior of the mean-squared displacement (44). On the other hand, for  $D_T > 0$  and in the long-time regime, the thermal fluctuations overcome the long-ranged correlations of the swimming velocity induced by the memory function. Therefore, the effective temperature of the resulting diffusive process exactly equals the temperature  $T$  of the bath regardless of  $v_0$ , see Eq. (45).

#### IV. SUMMARY AND FINAL REMARKS

In this work, we have investigated a generalization of the so-called active Ornstein-Uhlenbeck model for the motion of self-propelled particles subject to both thermal and nonequilibrium active fluctuations. The model considered here is based on the generalized Langevin equation (1b) for the swimming velocity and incorporates different channels of persistence of the particle swimming velocity by means of a memory function and additive colored noise. We have explicitly obtained the joint probability density of the particle position and its swimming velocity for the complete process.

We have also shown that such a probability density can be split into a thermally diffusive component and an active one. The latter satisfies the Fokker-Planck equation (16), which explicitly involves the time-dependent elements of the active covariance matrix.

We have obtained numerical and analytical results for the velocity autocorrelation function and the mean-squared displacement for two specific memory functions that arise in many natural systems: a finite-ranged exponential decay and a long-ranged power law. In both cases, damped-oscillatory behavior, that alternates between positive and negative correlations, of the swimming velocity emerges for certain values of the relevant parameters. The oscillations are damped in the case of the exponential decay, which leads to the emergence of an active diffusion coefficient and allows the definition of a nonequilibrium effective temperature. In contrast, oscillations are long lived for the power-law memory, and, remarkably, long-time subdiffusion is observed. This provides a simple example of free self-propelled motion where the concept of nonequilibrium effective temperature can not be trivially applied.

Although the effects of exponential memory have already been explicitly considered on the rotational motion of active Brownian particles [47,55,72,73], to our knowledge this is the first time that a general formulation encompassing long-lived correlations in the swimming speed has been studied. Our approach has allowed us to uncover numerous patterns of active motion which are absent in the conventional AOUM. Therefore, we expect that our results will be relevant for the understanding and modeling of intricate active systems, whose underlying dynamics, caused either by internal or external mechanisms, give rise to strong memory effects. In fact, our single-particle model is able to qualitatively capture a variety of behaviors observed in numerous active systems where long-range memory in the swimming velocity emerges either from self- or interparticle interactions. Similar effects are also expected to happen for deformable, asymmetric, or chiral self-propelled particles swimming in non-Newtonian fluid environments. Under such conditions, the local rheological properties of the medium, coupled to the response of the particle, can result in strongly correlated

fluctuations of the propulsion velocity. A further step will be to investigate the effect of confining potentials and external flows, as they introduce additional timescales and correlations that could significantly modify the persistence of the active motion.

#### ACKNOWLEDGMENT

F.J.S. kindly acknowledges support from DGAPA, UNAM-PAPIIT-IN114717.

#### APPENDIX: DERIVATION OF THE ACTIVE FOKKER-PLANCK EQUATION

We briefly derive the Fokker-Planck equation (16) for the bivariate probability density,  $G_{\text{act}}^2(x, v_s, t)$ , that corresponds to the active part of motion. The starting point is the characteristic function  $\hat{G}_{\text{act}}^{(2)}(k, q, t)$  of active motion, given by Eq. (8b). After applying the advective derivative in Fourier space,  $\frac{\partial}{\partial t} - k \frac{\partial}{\partial q}$ , to the expression (8b) we have that

$$\begin{aligned} & \left( \frac{\partial}{\partial t} - k \frac{\partial}{\partial q} \right) \hat{G}_{\text{act}}^{(2)}(k, q, t) \\ &= -qk \left[ \frac{d}{dt} \sigma_{v_s v_s}^2(t) - \sigma_{xv_s}^2(t) \right] \hat{G}_{\text{act}}^{(2)}(k, q, t) \\ & \quad - q^2 \left[ \frac{1}{2} \frac{d}{dt} \sigma_{v_s v_s}^2(t) \right] \hat{G}_{\text{act}}^{(2)}(k, q, t), \end{aligned} \quad (\text{A1})$$

where  $\sigma_{v_s v_s}^2(t)$ ,  $\sigma_{xv_s}^2(t)$ , and  $\sigma_{xx}^2(t)$  are the elements of the active covariance matrix  $\Sigma_{\text{act}}$ , and we have used that  $\sigma_{xv_s}^2(t) = \frac{1}{2} \frac{d}{dt} \sigma_{xx}^2(t)$ , which makes the proportional terms to  $k^2$  cancel each other. By noticing that

$$\begin{aligned} qk \hat{G}_{\text{act}}^{(2)}(k, q, t) &= - \frac{1}{\sigma_{xv_s}^2(t)} q \frac{\partial}{\partial q} \hat{G}_{\text{act}}^{(2)}(k, q, t) \\ & \quad - q^2 \frac{\sigma_{v_s v_s}^2(t)}{\sigma_{xv_s}^2(t)} \hat{G}_{\text{act}}^{(2)}(k, q, t), \end{aligned} \quad (\text{A2})$$

(as can be checked straightforwardly by direct substitution), we have that Eq. (A1) can be rewritten as

$$\begin{aligned} & \left( \frac{\partial}{\partial t} + k \frac{\partial}{\partial q} \right) \hat{G}_{\text{act}}^{(2)}(k, q, t) \\ &= - \left[ f(t)q \frac{\partial}{\partial q} + g(t)qk + h(t)q^2 \right] \hat{G}_{\text{act}}^{(2)}(k, q, t), \end{aligned} \quad (\text{A3})$$

whose inverse Fourier transform directly leads to the Fokker-Planck equation (16), with  $f(t)$ ,  $g(t)$ , and  $h(t)$  as given in Eqs. (17).

- 
- [1] J. Taktikos, H. Stark, and V. Zaburdaev, *PLoS ONE* **8**, e81936 (2013).
- [2] K. M. Taute, S. Gude, S. J. Tans, and T. S. Shimizu, *Nat. Commun.* **6**, 8776 (2015).
- [3] C. Bechinger, R. Di Leonardo, H. Löwen, C. Reichhardt, G. Volpe, and G. Volpe, *Rev. Mod. Phys.* **88**, 045006 (2016).
- [4] S. Ramaswamy, *Annu. Rev. Condens. Matter Phys.* **1**, 323 (2010).
- [5] M. C. Marchetti, J. F. Joanny, S. Ramaswamy, T. B. Liverpool, J. Prost, M. Rao, and R. A. Simha, *Rev. Mod. Phys.* **85**, 1143 (2013).
- [6] J. R. Howse, R. A. L. Jones, A. J. Ryan, T. Gough, R. Vafabakhsh, and R. Golestanian, *Phys. Rev. Lett.* **99**, 048102 (2007).
- [7] J. Palacci, C. Cottin-Bizonne, C. Ybert, and L. Bocquet, *Phys. Rev. Lett.* **105**, 088304 (2010).
- [8] H.-R. Jiang, N. Yoshinaga, and M. Sano, *Phys. Rev. Lett.* **105**, 268302 (2010).
- [9] W. Gao, R. Dong, S. Thamphiwatana, J. Li, W. Gao, L. Zhang, and J. Wang, *ACS Nano* **9**, 117 (2015).
- [10] J. R. Gomez-Solano, S. Samin, C. Lozano, P. Ruedas-Batuecas, R. van Roij, and C. Bechinger, *Sci. Rep.* **7**, 14891 (2017).
- [11] S. C. Takatori, W. Yan, and J. F. Brady, *Phys. Rev. Lett.* **113**, 028103 (2014).
- [12] F. Ginot, I. Theurkauff, D. Levis, C. Ybert, L. Bocquet, L. Berthier, and C. Cottin-Bizonne, *Phys. Rev. X* **5**, 011004 (2015).
- [13] S. C. Takatori and J. F. Brady, *Phys. Rev. E* **91**, 032117 (2015).
- [14] H. Oukris and N. E. Israeloff, *Nat. Phys.* **6**, 135 (2010).
- [15] J. Colombani, L. Petit, C. Ybert, and C. Barentin, *Phys. Rev. Lett.* **107**, 130601 (2011).
- [16] E. Dieterich, J. Camunas-Soler, M. Ribezzi-Crivellari, U. Seifert, and F. Ritort, *Nat. Phys.* **11**, 971 (2015).
- [17] D. Loi, S. Mossa, and L. F. Cugliandolo, *Phys. Rev. E* **77**, 051111 (2008).
- [18] J. Tailleur and M. E. Cates, *Europhys. Lett.* **86**, 60002 (2009).
- [19] M. Enculescu and H. Stark, *Phys. Rev. Lett.* **107**, 058301 (2011).
- [20] E. Ben-Isaac, Y. K. Park, G. Popescu, F. L. H. Brown, N. S. Gov, and Y. Shokef, *Phys. Rev. Lett.* **106**, 238103 (2011).
- [21] D. Loi, S. Mossa, and L. F. Cugliandolo, *Soft Matter* **7**, 3726 (2011).
- [22] G. Szamel, *Phys. Rev. E* **90**, 012111 (2014).
- [23] D. Levis and L. Berthier, *Europhys. Lett.* **111**, 60006 (2015).
- [24] F. J. Sevilla, A. V. Arzola, and E. P. Cital, *Phys. Rev. E* **99**, 012145 (2019).
- [25] G. Szamel, E. Flenner, and L. Berthier, *Phys. Rev. E* **91**, 062304 (2015).
- [26] U. M. B. Marconi, and C. Maggi, *Soft Matter* **11**, 8768 (2015).
- [27] E. Fodor, C. Nardini, M. E. Cates, J. Tailleur, P. Visco, and F. van Wijland, *Phys. Rev. Lett.* **117**, 038103 (2016).
- [28] T. F. F. Farage, P. Krinninger, and J. M. Brader, *Phys. Rev. E* **91**, 042310 (2015).
- [29] S. Das, G. Gompper, and R. G. Winkler, *New J. Phys.* **20**, 015001 (2018).
- [30] L. Caprini, U. M. B. Marconi, and A. Vulpiani, *J. Stat. Mech.: Theory Exp.* (2018) 033203.
- [31] D. Mandal, K. Klymko, and M. R. DeWeese, *Phys. Rev. Lett.* **119**, 258001 (2017).

- [32] U. M. B. Marconi, A. Puglisi, and C. Maggi, *Sci. Rep.* **7**, 46496 (2017).
- [33] A. Puglisi, and U. M. B. Marconi, *Entropy* **19**, 356 (2017).
- [34] R. Kubo, *Rep. Prog. Phys.* **29**, 255 (1966).
- [35] R. F. Fox, *J. Math. Phys.* **18**, 2331 (1977).
- [36] K. Wang and M. Tokuyama, *Physica A* **265**, 341 (1999).
- [37] N. Pottier, *Physica A* **317**, 371 (2003).
- [38] A. D. Viñales and M. A. Despósito, *Phys. Rev. E* **75**, 042102 (2007).
- [39] M. A. Despósito and A. D. Viñales, *Phys. Rev. E* **77**, 031123 (2008).
- [40] M. A. Desposito, and A. D. Viñales, *Phys. Rev. E* **80**, 021111 (2009).
- [41] R. F. Camargo, E. C. de Oliveira, and J. V. Jr., *J. Math. Phys.* **50**, 123518 (2009).
- [42] T. Sandev and Z. Tomovski, *Phys. Scr.* **82**, 065001 (2010).
- [43] T. Sandev, R. Metzler, and Z. Tomovski, *J. Math. Phys.* **55**, 023301 (2014).
- [44] A. E. Patteson, A. Gopinath, M. Goulian, and P. E. Arratia, *Sci. Rep.* **5**, 15761 (2015).
- [45] D. E. Schamel, A. G. Mark, J. G. Gibbs, C. Miksch, K. I. Morozov, A. M. Leshansky, and P. Fischer, *ACS Nano* **8**, 8794 (2014).
- [46] J. R. Gomez-Solano, A. Blokhuis, and C. Bechinger, *Phys. Rev. Lett.* **116**, 138301 (2016).
- [47] N. Narinder, C. Bechinger, and J. R. Gomez-Solano, *Phys. Rev. Lett.* **121**, 078003 (2018).
- [48] S. Henkes, Y. Fily, and M. C. Marchetti, *Phys. Rev. E* **84**, 040301(R) (2011).
- [49] O. Chepizhko, and F. Peruani, *Phys. Rev. Lett.* **111**, 160604 (2013).
- [50] A. Morin, D. Lopes Cardozo, V. Chikkadi, and D. Bartolo, *Phys. Rev. E* **96**, 042611 (2017).
- [51] J. Taktikos, V. Zaburdaev, and H. Stark, *Phys. Rev. E* **84**, 041924 (2011).
- [52] M. Suga, S. Suda, M. Ichikawa, and Y. Kimura, *Phys. Rev. E* **97**, 062703 (2018).
- [53] F. J. Sevilla, *The Non-equilibrium Nature of Active Motion* (Springer International Publishing, Cham, 2018), pp. 59–86.
- [54] The equilibrium situation, where the autocorrelation function of the noise and the memory function  $\gamma(t)$  are correctly related by  $k_B T$ , has been extensively studied within the context of free and confined passive Brownian motion [36–43].
- [55] P. K. Ghosh, Y. Li, G. Marchegiani, and F. Marchesoni, *J. Chem. Phys.* **143**, 211101 (2015).
- [56] K. G. Wang, *Phys. Rev. A* **45**, 833 (1992).
- [57] K. S. Fa, *Eur. Phys. J. B* **65**, 265 (2008).
- [58] C. Wilhelm, F. Gazeau, and J.-C. Bacri, *Phys. Rev. E* **67**, 061908 (2003).
- [59] A. Ochab-Marcinek, S. A. Wieczorek, N. Ziębacz, and R. Hołyst, *Soft Matter* **8**, 11173 (2012).
- [60] E. Sarmiento-Gomez, D. Lopez-Diaz, and R. Castillo, *J. Phys. Chem. B* **114**, 12193 (2010).
- [61] J. R. Gomez-Solano, and C. Bechinger, *New J. Phys.* **17**, 103032 (2015).
- [62] S. Paul, B. Roy, and A. Banerjee, *J. Phys.: Condens. Matter* **30**, 345101 (2018).
- [63] R. Großmann, F. Peruani, and M. Bär, *New J. Phys.* **18**, 043009 (2016).
- [64] F. J. Sevilla, [arXiv:1905.07090](https://arxiv.org/abs/1905.07090) [cond-mat.stat-mech] (2019).
- [65] R. F. Rodriguez, J. Fujioka, and E. Salinas-Rodriguez, *Physica A* **427**, 326 (2015).
- [66] I. M. Tolic-Norrelykke, E. L. Munteanu, G. Thon, L. Oddershede, and K. Berg-Sorensen, *Phys. Rev. Lett.* **93**, 078102 (2004).
- [67] M. Bolland, N. Desprat, D. Icard, S. Féréol, A. Asnacios, J. Browaeys, S. Hénon, and F. Gallet, *Phys. Rev. E* **74**, 021911 (2006).
- [68] Y. Kobayashi, M. Tsukune, T. Miyashita, and M. G. Fujie, *Phys. Rev. E* **95**, 022418 (2017).
- [69] H. Qian, in *Processes with Long-Range Correlations: Theory and Applications*, edited by G. Rangarajan and M. Z. Ding, Lecture Notes in Physics Vol. 621 (Springer-Verlag, Berlin, Heidelberg, 2003), pp. 22–33.
- [70] K. Diethelm, N. J. Ford, and A. D. Freed, *Nonlinear Dyn.* **29**, 3 (2002).
- [71] C. R. Dietrich and G. N. Newsam, *SIAM J. Sci. Comput.* **18**, 1088 (1997).
- [72] F. Peruani and L. G. Morelli, *Phys. Rev. Lett.* **99**, 010602 (2007).
- [73] C.-T. Hu, J.-C. Wu, and B.-Q. Ai, *J. Stat. Mech.: Theory Exp.* (2017) 053206.